

# Synthesis of hexagonal and cubic super-microporous niobium phosphates with anion exchange capacity and catalytic properties

Nawal Kishor Mal and Masahiro Fujiwara\*

National Institute of Advanced Industrial Science and Technology (AIST) Kansai, 1-8-31 Midorigaoka, Ikeda, Osaka 563-8577, Japan. E-mail: m-fujiwara@aist.go.jp

Received (in Cambridge, UK) 14th August 2002, Accepted 3rd October 2002

First published as an Advance Article on the web 18th October 2002

Super-microporous hexagonal niobium phosphate synthesized using neutral surfactant ( $S^{O}I^0$  mechanism) and cubic structure with cationic surfactant ( $S^+X^-I^+$ ); the hexagonal niobium phosphate possesses an excellent anion exchange capacity ( $6.3 \text{ mmol g}^{-1}$ ) and high product selectivity towards 4-naphthaquinone (88.6%) in the oxidation of 1-naphthol in presence of aqueous  $H_2O_2$ .

Discovery of M41S silicates by Mobil scientists in 1992<sup>1</sup> has stimulated considerable interests in this new class of mesoporous materials. Subsequently, a variety of transition metal oxides and a few non-lamellar transition metal (Ti, Zr, Fe and V) phosphate<sup>2,3</sup> mesoporous molecular sieves have been synthesized, through self-assembly of inorganic precursors and surfactants into supramolecular aggregates.<sup>2-4</sup> Recently, synthesis of mesoporous tin phosphates using a long chain alkyltrimethylammonium bromide has been reported.<sup>5</sup> Phosphate-based molecular sieves with mostly neutral frameworks have attracted considerable attention of academia and industry.<sup>6</sup> Commercial anion exchangers are mostly organic based, such as anion-exchange resins. Cation-exchange materials are very common for inorganic materials (e.g. zeolites),<sup>7</sup> whereas anion-exchangeable inorganic materials are rarely reported in the literature. Hydrotalcite,<sup>8</sup> mesoporous titanium phosphate<sup>2a</sup> and an aluminophosphate derived from a polyoxometalate cluster<sup>9</sup> are the only examples of such materials.

All reported non-lamellar mesoporous transition metal phosphates have been synthesized through the  $S^+I^-$ ,  $S^-I^+$  or  $S^+X^-I^+$  mechanism (where S = surfactant, I = inorganic species and X = counter ions).<sup>2,3</sup> Moreover, in the synthesis of mesoporous transition metal phosphates, equimolar amounts of the metal source and phosphoric acid have been used, therefore the possibility of reproducibility of the metal to phosphorus ratio in the product is uncertain.

Herein we describe, for the first time, (a) use of the hydrogen bonding mechanism ( $S^{O}I^0$ ) to synthesize novel super-microporous transition metal (niobium) phosphate with high anion exchange capacity using hexadecyl amine (HDA) as surfactant and (b) formation of niobium phosphate with cubic structure using hexadecyltrimethylammonium bromide (CTMABr) ( $S^+X^-I^+$ ).

In a typical synthesis, 2.73 g of  $NbCl_5$  (10 mmol) was partially hydrolyzed with 50 g of  $H_2O$ . 2.30 g of  $H_3PO_4$  (20 mmol) was then added, which caused a vigorous reaction. 50 g of  $H_2O$  was then added and the reaction mixture stirred for 30 min. Aqueous ammonia was added until the pH reached 2.60. The resulting precipitate was filtered off and washed with distilled water several times to remove excess chloride ions. 10 g of  $H_2O$  and 1.45 g of HDA (6 mmol) was added to the precipitate in a plastic beaker and stirred for 30 min. Finally, the required amount of  $H_3PO_4$  (0.92 g, 8 mmol) was added, with the pH maintained at 3.88 under stirring for 30 min. The gel was heated in a Teflon lined stainless steel autoclave at 65 °C under autogeneous pressure for 2 days. The final product was filtered off, washed with distilled water, dried at 100 °C and calcined at 450 °C for 6 h. This sample is referred to as NbPO-1H. In another typical procedure using CTMABr as surfactant, 34.6 g of  $H_3PO_4$  (300 mmol) was added to 2.73 g of  $NbCl_5$  (10 mmol)

in 40 g of  $H_2O$  followed by the addition of 1.82 g of CTMABr (5 mmol) under stirring for 15 min. Finally, heating in a Teflon-lined stainless steel autoclave at 90 and 150 °C for 1 and 2 days, respectively gave the crystalline product which was filtered off, washed, and dried at 100 °C for 1 day. This sample is referred as NbPO-2C.

Elemental analyses of the samples were carried out using ICP (Shimadzu ICPV-1017). Characterization of the samples was obtained using XRD (Cu-K $\alpha$  radiation,  $\lambda = 0.15406 \text{ nm}$ ), TEM and  $N_2$  sorption at 77 K. The anion exchange capacity of the niobium phosphate was evaluated by potentiometric titration of the filtrates obtained on treatment of calcined NbPO-1H with aqueous  $NH_3$ . The filtrate was titrated against aqueous  $AgNO_3$  solution and a known concentration of oxalic acid in the presence of phenolphthalein as indicator. The catalytic activity of the niobium phosphate sample was tested in the hydroxylation of 1-naphthol, batchwise in a round bottom flask in the presence of aqueous  $H_2O_2$  (30 wt%) as oxidant. The products were analyzed using GC (GC-17A, Shimadzu) using a capillary column and confirmed by standard product and GC-MS.

The XRD pattern of the as-synthesized NbPO-1H shows three reflections at low angles similar to those recorded for MCM-41 (Fig. 1(a)). These reflections can be indexed as (100), (110) and (200), assuming hexagonal unit. All the reflections appear below 6° as expected; however the (110) and (200) peaks are not well resolved. This effect was observed previously in samples of MSU-1 silica, and has been attributed to the small particle size and/or the regions of local disorder.<sup>10</sup> The structure of NbPO-1H after calcination at 450 °C for 6 h retained its structure and showed areflection at (100) (Fig. 1(b)). The XRD pattern of NbPO-2C is cubic<sup>11</sup> with an intense reflection at (200) and weak reflections at (210), (211) and (321) as shown in Fig. 1(c). TEM images of calcined NbPO-1H and as-synthesized NbPO-2C are shown in Fig. 2. The TEM image of calcined NbPO-1H confirms the presence of ac distorted

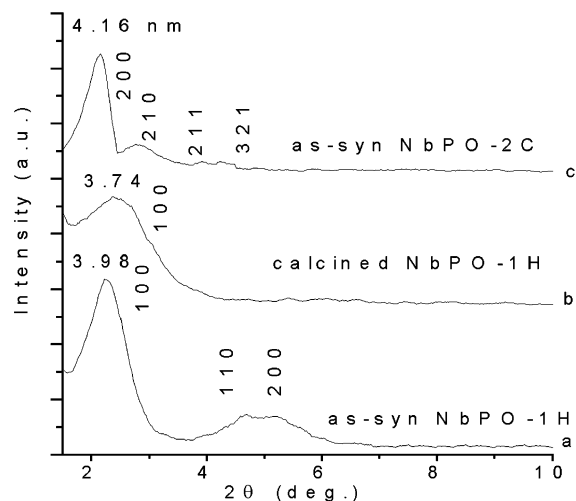
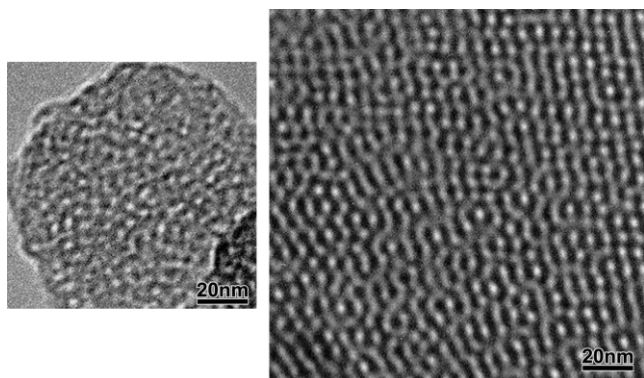


Fig. 1 XRD profiles of as-synthesized NbPO-1H (a), calcined NbPO-1H (b) and as-synthesized NbPO-2C (c).



**Fig. 2** TEM images of calcined NbPO-1H (left) and as-synthesized NbPO-2C (right).

hexagonal structure.<sup>10</sup> The TEM image of NbPO-2C shows the organized cubic structure.<sup>11</sup>

The BET specific surface area and pore volume of calcined NbPO-1H are 482 m<sup>2</sup>g<sup>-1</sup> and 0.35 cm<sup>3</sup>g<sup>-1</sup>, respectively. The surface area and pore volume of mesoporous titanium phosphate are higher (740 m<sup>2</sup>g<sup>-1</sup> and 0.79 cm<sup>3</sup>g<sup>-1</sup>, respectively)<sup>2a,b</sup> than for other metal ions.<sup>2</sup> Mesoporous iron and tin phosphate have lower surface area (230 to 425 m<sup>2</sup>g<sup>-1</sup>) and pore volume (0.21 cm<sup>3</sup>g<sup>-1</sup>).<sup>2d,5</sup> Fig. 3 shows the N<sub>2</sub> sorption isotherm, pore size distribution and UV-VIS spectrum of NbPO-1H. The adsorption-desorption isotherms are of type I and do not show hysteresis loops (Fig. 3A). Schüth and coworkers observed similar isotherms with mesoporous titanium oxo phosphate and explain this through the presence of ‘supermicropores’ within the 1.5–2.0 nm range.<sup>12</sup> The pore size distribution curve shows a narrow pore size distribution with peak pore diameter at 1.66 nm (Fig. 3A, inset). In contrast, the average pore diameter reported for other transition metal phosphates are in the range 2.3–3.0 nm.<sup>2</sup> The UV-VIS spectra of as-synthesized and calcined NbPO-1H show the presence of a peak at 263 nm and absence of peak at 308 nm, whereas mesoporous niobium oxide shows a peak at 308 nm (octahedral species). This indicates that niobium ions in NbPO-1H are tetra- or penta-coordinated and not hexa-coordinated.

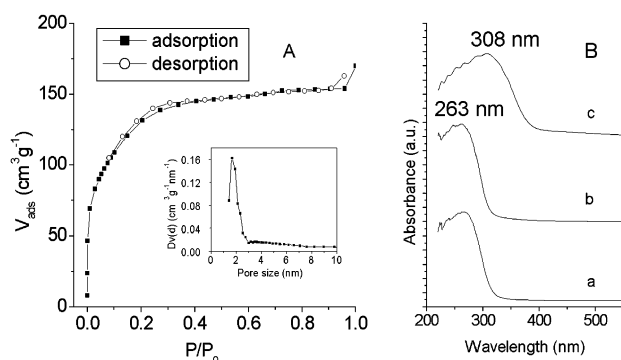


**Fig. 3** (A) N<sub>2</sub> adsorption-desorption isotherms of calcined NbPO-1H. (Inset: Pore size distribution curve from the adsorption branch of the isotherm) and (B) UV-VIS spectra of as-synthesized NbPO-1H (a), calcined NbPO-1H (b) and mesoporous niobium oxide (c).

**Table 1** Catalytic activity in the oxidation of 1-naphthol

Catalyst	Conversion (mol %)	H <sub>2</sub> O <sub>2</sub> efficiency (mol%)	Product distribution (mol%) <sup>a</sup>		
			1,2-one	1,4-one	Others <sup>b</sup>
NbPO-1H	9.1	52.4	9.4	82.7	7.9

<sup>a</sup> Conversion = mol% of 1-naphthol consumed during the reaction, H<sub>2</sub>O<sub>2</sub> efficiency = mol% of H<sub>2</sub>O<sub>2</sub> consumed in the formation of 1,2-one (1,2-naphthaquinone), 1,4-one (1,4-naphthaquinone) and others. <sup>b</sup> Others includes the formation of 1,2-dihydroxy naphthalene, 1,4-dihydroxynaphthalene, 1,6-dihydroxynaphthalene and 1,6-naphthaquinone.

P/Nb molar ratios in the samples NbPO-1H and NbPO-2C are 1.13 and 1.28, respectively. The double positive charge of the framework is balanced by the presence of excess phosphorous ions (e.g. H<sub>2</sub>PO<sub>4</sub><sup>-</sup> and HPO<sub>4</sub><sup>2-</sup>) and Cl<sup>-</sup> ions. The anion exchange capacity of calcined NbPO-1H is 6.3 mmol g<sup>-1</sup>. The value is higher than those of other well-known anion-exchangers, such as ion exchange resins (1–4 mmol g<sup>-1</sup>), mesoporous aluminophosphate (1–4 mmol g<sup>-1</sup>) and titanium phosphate (5.4 mmol g<sup>-1</sup>).<sup>2a,9</sup> This suggests that anion exchange capacity of niobium phosphate is generated in the framework due to incorporation of Nb and P atoms.

The catalytic activity of calcined NbPO-1H in the hydroxylation of 1-naphthol is presented in Table 1. The 1-naphthol conversion (mol% 1-naphthol consumed) and H<sub>2</sub>O<sub>2</sub> efficiency are 9.1 and 52.4%, respectively. H<sub>2</sub>O<sub>2</sub> efficiency is defined as mol% of H<sub>2</sub>O<sub>2</sub> consumed in the formation of 1,2-naphthaquinone, 1,4-naphthaquinone and other products. These include the 1,2-dihydroxynaphthalene, 1,4-dihydroxynaphthalene, 1,6-dihydroxynaphthalene and 1,6-naphthaquinone. Interestingly, the product distribution shows that hydroxylation of 1-naphthol take place selectively at the *para* position of the aromatic ring. Product selectivity of 1,2-naphthaquinone, 1,4-naphthaquinone and others are 9.4, 82.7 and 7.9%, respectively. At the beginning of the reaction, primary oxidation products such as 1,2-dihydroxynaphthalene, 1,4-dihydroxynaphthalene and 1,6-dihydroxynaphthalene were formed, which were further oxidized to the corresponding ketones 1,2-naphthaquinone, 1,4-naphthaquinone and 1,6-naphthaquinone, respectively. The unusual phenomenon of high selectivity towards 1,4-naphthaquinone (*para* isomer) over niobium phosphate is not clear. However, this clearly evidenced that niobium ions in the framework catalyzed selective hydroxylation at the *para* position of the 1-naphthol ring.

## Notes and references

- C. T. Kresge, M. E. Leonowicz, W. J. Roth, J. C. Vartuli and J. S. Beck, *Nature*, 1992, **359**, 710–714.
- (a) A. Bhaumik and S. Inagaki, *J. Am. Chem. Soc.*, 2001, **123**, 691–696; (b) D. J. Jones, G. Aptel, M. Brandhorst, M. Jacquin, J. J. Jiménez, A. J. López, P. M. Torres, I. Piwonski, E. R. Castellón, J. Zajac and J. Rozière, *J. Mater. Chem.*, 2000, **10**, 1957–1963; (c) J. J. Jiménez, P. M. Torres, P. O. Pastor, E. R. Castellón, A. J. López, D. J. Jones and J. Rozière, *Adv. Mater.*, 1998, **10**, 812–815; (d) X. Guo, W. Ding, X. Wang and Q. Yan, *Chem. Commun.*, 2001, 709–710.
- (a) T. Abe, A. Taguchi and M. Iwamoto, *Chem. Mater.*, 1995, **7**, 1429–1430; (b) T. Doi and T. Miyake, *Chem. Commun.*, 1996, 1635–1636; (c) N. Mizuno, H. Hatayama, S. Uchida and A. Taguchi, *Chem. Mater.*, 2001, **13**, 179–184.
- J. Y. Ying, C. P. Mehnert and M. S. Wong, *Angew. Chem., Int. Ed.*, 1999, **38**, 56–77.
- C. Serre, A. Auroux, A. Gervasini, M. Hervieu and G. Férey, *Angew. Chem., Int. Ed.*, 2002, **41**, 1594–1597; N. K. Mal, S. Ichikawa and M. Fujiwara, *Chem. Commun.*, 2001, 212–213.
- (a) S. T. Wilson, M. M. Lok, C. A. Messina, T. R. Cannan and E. M. Flanigen, *J. Am. Chem. Soc.*, 1982, **104**, 1146–1147; (b) M. E. Davis, C. Saldarriaga, C. Montes, J. Garces and C. Crowder, *Nature*, 1988, **331**, 698–699; (c) S. Serre and G. Férey, *J. Mater. Chem.*, 1999, **9**, 579–585.
- (a) R. M. Barrer, *Hydrothermal Chemistry of Zeolites*, Academic Press, New York, 1982; (b) A. Corma, *Chem. Rev.*, 1997, **97**, 2373–2419.
- T. Matsushita, K. Ebitani and K. Kaneda, *Chem. Commun.*, 1999, 265–266.
- (a) B. T. Holland, P. K. Isbester, C. F. Blanford, E. G. Munson and A. Stein, *J. Am. Chem. Soc.*, 1997, **119**, 6796–6803; (b) D. A. Kron, B. T. Holland, R. Wipson, C. Maleke and A. Stein, *Langmuir*, 1999, **15**, 8300–8308.
- S. A. Bagshaw, E. Prouzet and T. J. Pinnavaia, *Science*, 1995, **269**, 1242–1244.
- A. monnier, F. Schuth, Q. Huo, D. Kumar, D. Margolese, R. S. Maxwell, G. D. Stucky, M. Krishnamurthy, P. Petroff, A. Firouzi, M. Janicke and B. F. Chmelka, *Science*, 1993, **261**, 1299–1303.
- M. Thieme and F. Schuth, *Microporous Mesoporous Mater.*, 1999, **27**, 193–200.